

# HALLOYSITE AND KAOLINITE: TWO CLAY MINERALS WITH GEOLOGICAL AND TECHNOLOGICAL IMPORTANCE

Blanca Bauluz Lázaro

Departamento de Ciencias de la Tierra

Facultad de Ciencias

Universidad de Zaragoza

bauluz@unizar.es

*Premio a la Investigación de la Academia 2015. Sección de Naturales*

## **Abstract**

Halloysite and kaolinite have many similarities in structure, composition, and genesis. Both minerals are dioctahedral 1:1 layer silicates and are hydrated aluminium-silicates. Halloysite has the same theoretical chemical composition as kaolinite except for its higher water content because unit layers in halloysite are separated by a monolayer of water molecules. Halloysite has two forms, a more hydrous form with a single layer of water between the 1:1 layers, which is named halloysite-(10 Å), and a less hydrous form, termed halloysite-(7 Å). The presence or lack of water layers produces different basal spacings in the structure. The ideal unit formula for kaolinite is  $\text{Al}_2\text{Si}_2\text{O}_5(\text{OH})_4$  and  $\text{Al}_2\text{Si}_2\text{O}_5(\text{OH})_4 \cdot n\text{H}_2\text{O}$ , where  $n = 0$  for halloysite-(7 Å) and  $n = 2$  for halloysite-(10 Å), respectively. Halloysite and kaolinite show variable  $\text{Fe}^{3+}$  contents in octahedral positions, and this substitution can be greater in halloysite (up to 12.8% of  $\text{Fe}_2\text{O}_3$ ) than in kaolinite (up to 7% of  $\text{Fe}_2\text{O}_3$ ). Kaolinite usually shows platy morphology and halloysite may display tubular, spheroidal, or platy morphologies. The variations in halloysite morphology appear to be related to crystallization conditions and geological occurrences. Halloysite and kaolinite form under low-temperature conditions and are abundant phases in soils and in weathered and hydrothermally altered rocks. They frequently occur together. During these alterations, some phases of the parent rocks (volcanic glass, feldspars, and

phyllosilicates) are dissolved, and halloysite and kaolinite crystallize from solutions. Under weathering conditions, halloysite and kaolinite are associated with warm and humid climates and their occurrence in the geological record may be related with specific climate conditions (e.g. the Paleocene/Eocene boundary and Lower Cretaceous (Wealden) sediments). Under hydrothermal alteration, the crystallization of halloysite and kaolinite is related to moderately acid hydrothermal solutions. Kaolinite usually needs higher temperatures ( $> 100^{\circ}\text{C}$ ) than halloysite ( $< 100^{\circ}\text{C}$ ) to crystallize. Deposits of halloysite and/or kaolinite of economic interest can be formed both by weathering and hydrothermal alterations. Their physical properties make them suitable for very interesting technological applications. Kaolinite is a very important industrial mineral (e.g. in paper, ceramics, and refractory manufacturing, in zeolite synthesis, etc.), and halloysite is becoming increasingly important due mainly to its use in nanotechnology applications, which take advantage of its tubular habits (e.g. for capturing compounds, for controlled release, and to produce delivery systems).

## 1 Introduction

Kaolinite and halloysite are two clay minerals with significant and increasing importance because of their structure, composition, genesis conditions, and applications. The specific conditions in which they form make them useful in climate change reconstructions and, because of their structure and composition, they have a large number of industrial applications that are increasing with research.

Kaolinite and halloysite belong to the phyllosilicate group and tend to have a sheet structure. As with many other phyllosilicates, they are usually micron or submicron in size. To describe this characteristic size in phyllosilicates, the term *clay mineral* was coined. Compositionally, kaolinite and halloysite (like many clay minerals) are hydrated aluminium silicates. In nature, they are associated to other minerals, including zeolites, quartz and oxide minerals, as well as lesser amounts of all the other minerals. Their preferential formation is under surface (alterites, soils, sediments) or subsurface (diagenesis, hydrothermal alterations) conditions. All these environments are characterized by low temperatures, with clay minerals occurring in the range of  $4 - 200^{\circ}\text{C}$ .

In general, low-temperature environments in which kaolinite and halloysite are present display complex mineral assemblages and compositions, consisting of mixtures of clay minerals, non-clay phases, and even amorphous components that complicate their characterization and identification. X-ray diffraction (XRD) in combination with other techniques (e.g. infrared, Raman, EXAFS, NMR spectroscopies, etc.) allows mineralogists to identify clays and infer their structure and composition. The use of scanning and transmission electron microscopy (SEM, TEM) is also essential to analyse textural relations among the phases and individual particles to derive information on their crystal structure,

chemical composition, bonding state, and so on (Bauluz, 2007, 2013).

Although there is abundant literature focused on kaolinite and halloysite minerals, on many occasions there are discrepancies in nomenclature and identification most commonly due to the similarities between these phases. The aim of the paper is to review the major characteristics of halloysite and kaolinite as regards nomenclature and crystal chemistry, composition and morphology, genesis, and applications.

## 2 Phyllosilicate Structure

Phyllosilicate crystals fundamentally consist of silicon, aluminium or magnesium, oxygen, and hydroxyl (OH), with various associated cations according to the species. These ions and OH groups are organized into two-dimensional structures called sheets, occurring in two types: tetrahedral sheets and octahedral sheets.

Tetrahedral sheets have a general composition of  $T_2O_5$  (T = tetrahedral cation; mainly Si, with varying Al or  $Fe^{3+}$  contents). Silicon is located at the centre of the tetrahedron, and oxygen anions form the four corners. The individual tetrahedron shares three corners (the three basal oxygens) with adjacent tetrahedra, constituting a hexagonal mesh arrangement. The fourth tetrahedral corner points in a direction normal to the sheet. Its oxygen (the apical oxygen) forms part of the octahedral sheet.

The octahedral sheets comprise medium-sized cations at the centre of the octahedron (usually Al, Mg,  $Fe^{2+}$ , or  $Fe^{3+}$ ), and oxygens at the eight corners. The individual octahedra are linked laterally with the neighbouring octahedra, and vertically with the tetrahedra, by sharing oxygens. The smallest structural unit of the octahedral sheets contains three octahedra. If all three octahedra have cations at their centre (bivalent ions like  $Mg^{2+}$ ,  $Fe^{2+}$ ), the sheet is called trioctahedral. If only two octahedra are occupied and one octahedron is vacant (trivalent ions like  $Al^{3+}$ ,  $Fe^{3+}$ ), the sheet is dioctahedral.

The junction plane between the tetrahedral and octahedral sheets comprises the apical oxygens shared by the tetrahedra and the octahedra, plus unshared hydroxyls. The OH groups are located at the centre of each tetrahedral six-fold ring (hexagonal arrangement), at the same level as the apical oxygens.

The layered silicate structures are built up from different stacking combinations of these two basic sheets. In many layered silicates, there is a considerable substitution of Al for Si in the tetrahedral sites as well as of cations in octahedra, leading to a variation in mesh sizes. One consequence of a misfit between sheets is that, with some compositions, only very small crystals can grow as the strain imposed by any misfits will increase with the area of the layer. Clay minerals, in which this is the case, form a subgroup of layered silicates.

Phyllosilicates are classified by the way the layers are built up of tetrahedral and octa-



| Layered silicate type     | Group   | Characteristics  | Subgroup                       | Species examples                                     |
|---------------------------|---|--|--------------------------------|--|
| 1:1                       | kaolin-serpentine<br>no interlayers                       | $d_{001} = 7\text{\AA}$  | serpentine (tri)               | chrysotile,<br>antigorite, lizardite,<br>berthierine |
|                           |   |  | kaolin (di)                    | kaolinite, dickite,<br>nacrite, halloysite           |
| 2:1                       | pyrophyllite-talc   | no interlayer sites. $d_{001} = 9\text{\AA}$   | talc (tri)                     | talc   |
|                           | smectite  | with cations + $\text{H}_2\text{O}$ in interlayer sites. $d_{001} = 12 - 15\text{\AA}$ | pyrophyllite (di)              | pyrophyllite   |
|                           |   |  | montmorillonite (dioctahedral) | montmorillonite,<br>beidellite,<br>nontronite        |
|                           |   |  | saponite (trioctahedral)       | saponite, hectorite,<br>stevensite                   |
|                           | vermiculite   | with cations + $\text{H}_2\text{O}$ in interlayer sites. $d_{001} = 12 - 15\text{\AA}$ | dioctahedral                   | dioctahedral,  |
|                           |   |  | vermiculite                    | vermiculite  |
|                           |   |  | trioctahedral                  | trioctahedral  |
|                           | mica  | with cations in interlayer sites $d_{001} = 10\text{\AA}$                              | vermiculite                    | vermiculite  |
|                           |   |  | dioctahedral                   | muscovite,<br>paragonite, illite,<br>glauconite      |
|                           |   |  | trioctahedral                  | phlogopite, biotite,<br>lepidolite                   |
| brittle mica              | with cations in interlayer sites $d_{001} = 10\text{\AA}$ | trioctahedral  | margarita                      |  |
|                           |   | brittle micas  |                                |  |
|                           |   | trioctahedral  | clintonite                     |  |
| 2:1<br>(inverted ribbons) | palygorskite-sepiolite<br>(=fibrous clays)                | no interlayer sites  | palygorskites                  | palygorskite   |
|                           |   |  | sepiolites                     | sepiolite  |
| 2:1:1                     | chlorite  | $d_{001} = 14\text{\AA}$   | $d_{001} = 10.5\text{\AA}$     |  |
|                           |   |  | dioctahedral                   | donbassite   |
|                           |   |  | chlorites                      |  |
|                           |   |  | trioctahedral                  | clinochlore,<br>chamosite                            |
|                           |   |  | di, tri octahedral             | cookeite,<br>sudoite                                 |
|                           |   |  | chlorite                       |  |

Table 1: Classification of phyllosilicates.

### 3 Nomenclature and Structure

Kaolinite, halloysite with dicrite, and nacrite form the kaolin group. All of them are dioctahedral 1:1 layer silicates, with  $\text{Al}^{3+}$  in octahedral positions. As in all natural dioctahedral minerals, the vacant and occupied octahedral sites form a distorted hexagonal pattern in which each large vacancy is surrounded by six smaller occupied sites. Newnham in 1961 pointed out that enlargement of the vacant site is due to mutual repulsion between adjacent  $\text{Al}^{3+}$  cations and the concomitant movement of coordinating anions towards one another along the shared octahedral edges.

The triclinic nature of kaolinite ( $\text{Al}_2\text{Si}_2\text{O}_5(\text{OH})_4$ ) was suggested first by Brindley and Robinson (1945, 1946), who found that the indexing of X-ray powder patterns required a unit cell shape slightly distorted from the monoclinic geometry reported originally by Ross and Kerr (1931) from microscopic evidence and by Gruner (1932) from X-ray evidence. Brindley and Robinson, on the basis of better X-ray powder data, correctly determined that kaolinite instead must have a 1-layer structure in which adjacent layers are shifted by  $-a/3$ , that is, a dioctahedral modification of the 1M structure. Although vermicular macroscopic crystals of kaolinite exist, Mansfield and Mansley (1972) showed that these are always complexly intergrown by  $\pm 120^\circ$  pseudo-twin rotations around the normal layer and sometimes, in addition, by a  $180^\circ$  twin rotation around the  $x$  axis.

Honjo et al. (1954) proposed a triclinic layer arrangement for the structure of halloysite-(7 Å); however, on the basis of the SAED pattern, they deduced a monoclinic unit cell for halloysite-(7 Å) (Kohyama et al., 1978; Mitra & Bahattacherjee, 1975; Chukhorv & Zvyagin, 1966). Further, Kohyama et al. (1978) suggested a two-layer monoclinic structure with a Cc space group for both halloysite-(7 Å) and halloysite-(10 Å). The two-layer structure has been consistently observed in tubular halloysite (Chukhorv & Zvyagin, 1966; Kohyama et al. 1978; Noro, 1986). Bookin et al. (1989) studied the nature of stacking faults in kaolin-group minerals by analysing XRD profiles. They showed that a 1:1 layer structure, for a regular alternation of translations along the  $b$  axis, leads to a structure similar to that described by Chukhorv et al. (1966) for kaolinite. They suggested that the halloysite-like structure may be the end member of this defect-type kaolinite.

Mehnel (1935) recognized two different forms of halloysite, a less hydrous form with a composition near that of kaolinite [ $\text{Al}_2\text{Si}_2\text{O}_5(\text{OH})_4$ ] and with a basal spacing near 7.2 Å, and a more hydrous form with a composition near  $\text{Al}_2\text{Si}_2\text{O}_5(\text{OH})_4 \cdot 2\text{H}_2\text{O}$  and a basal spacing close to 10.1 Å. Mehnel (1935) used the terms *halloysite* and *metahalloysite* for the more hydrous and the less hydrous forms, respectively. Various nomenclature schemes have been suggested for the two forms of halloysite, which have resulted in considerable ambiguity. See Table 2 for the considered terms.

MacEwan (1947) suggested that *halloysite* be used in a general sense and prefixed appro-

| 1                                       | 2              | 3                        | 4   | 5          |
|---|----------------|--------------------------|---|------------|
| 7 Å-halloysite or<br>halloysite-(7 Å)   | metahalloysite | dehydrated<br>halloysite | halloysite                                | halloysite |
| 10 Å-halloysite or<br>halloysite-(10 Å) | halloysite     | halloysite               | hydrated halloysite or<br>hydrohalloysite | endellite  |

Table 2: Terms used for halloysites

priately for particular forms. The only unambiguous nomenclature is to indicate the basal spacing, as in the terms (1) in the table. It suffices to give the spacings with no higher precision than 7 Å and 10 Å although, in fact, there are some variations in the exact values. This is the nomenclature recommended by the AIPEA (Association Internationale pour l'Étude des Argiles).

The transformation of the 10 Å to the 7 Å form in atmospheres of controlled relative humidities was studied by Brindley and Goodyear (1948) by applying the treatment of Hendricks and Teller (1941) for diffraction by interstratified layer structures. The initial spacing of about 10 Å diminished to an average value of about 9.5 Å as a result of the interstratification of dehydrated layers. Between the 9.5 Å and the 7.9 Å stages, it was thought that mixtures were present. Aldrich and Carr (1972) followed the transformation in somewhat greater detail and are of the opinion that a continuous series of interstratified states exists between the 10 Å and 7 Å forms, each state being in equilibrium with the ambient atmosphere. The final reduction to the 7 Å state requires gentle heating. It is probably optimistic to consider that any clay mineral transformation proceeds in a wholly homogeneous manner because of the differences in particle size and form. Some particles may dehydrate more readily (or less readily) than others so that even if equilibrium is established, there are still differences between the precise state of dehydration reached by different particles.

Therefore, the structure of kaolinite and halloysite is the consequence of the stacking of tetrahedral and octahedral sheets (1:1 phyllosilicate) but, in the case of halloysite, the 1:1 unit layers are separated by a monolayer of water not present in kaolinite (Fig. 1). The presence of this layer of water produces a large basal spacing in the more hydrous halloysite form (10 Å), which easily distinguishes 10 Å halloysite from kaolinite that has a smaller spacing (7 Å). However, the identification of (7 Å)-halloysite is ambiguous because its diffraction and thermal patterns are almost identical with that of disordered kaolinite (Brindley, 1980). The most efficient and sensitive tools for identifying minerals of the kaolin subgroup are infrared (IR) and Raman spectroscopies (Frost, 1995, 1998; Frost & Vassallo, 1996; Frost et al., 1996; Frost & Shurvell, 1997). Each kaolin mineral exhibits a specific IR spectrum and presents distinct interactions to intercalation processes.

## 4 Chemical composition

Halloysite has the same theoretical chemical composition as kaolinite except for its higher water content. In halloysite, unit layers are separated by a monolayer of water molecules. The ideal unit formula for halloysite-(7 Å) and halloysite-(10 Å) is  $\text{Al}_2\text{Si}_2\text{O}_5(\text{OH})_4 \cdot n\text{H}_2\text{O}$ , where  $n = 0$  and 2, respectively (Bailey, 1988; Guggenheim & Eggleton, 1988). However, the chemical composition is subject to little variation. The common presence of impurities, such as associated clay minerals, Fe oxides, or poorly organized minerals (some of which may also be localized within halloysite tubes) in halloysitic and/or kaolinitic samples makes it difficult to assess their chemical composition (White & Dixon, 2002).

Chemical analyses of halloysites reveal variable and significant amounts (up to 12.8%) of  $\text{Fe}_2\text{O}_3$ . This finding may be due to the partial isomorphous substitution of  $\text{Fe}^{3+}$  for  $\text{Al}^{3+}$  in the octahedral sheet (Churchman & Theng, 1984; Wada & Mizota, 1982; Hart et al., 2002) or to physical mixtures with very fine iron oxides (e.g. hematite and goethite).

For a long time, kaolinite was considered to have no isomorphous substitution. In fact, detailed chemical analyses (Rengasamy et al., 1975; Lietard, 1977), electron microprobe analyses (Jepson & Rowse, 1975), Mossbauer spectroscopy (Komusinski et al., 1981; Fysh et al., 1983), ESR spectroscopy (Mestdagh et al., 1982; Brindley et al., 1986), infrared spectroscopy (Mendelovici et al., 1979), EXAFS spectroscopy (Bonnin et al., 1982), NMR spectroscopy (Stone & Torres-Sánchez, 1988), and more recently, electron paramagnetic resonance (Balan et al., 2007) show that small, variable amounts of iron (up to almost 3%  $\text{Fe}_2\text{O}_3$ ) can be accommodated within the octahedral sheet. Only occasionally have larger substitutions (up to 7% of  $\text{Fe}_2\text{O}_3$ ) been detected in kaolinites by scanning TEM (Petit & Decarreau, 1990).

## 5 Relation between morphology and crystal chemistry

The particle morphology of halloysite appears to be related to crystallization conditions and geological occurrences (Joussin et al., 2005 and references therein).

Spheroidal, tubular, and plate halloysite have been described (Fig. 2, 3). The diameter of spherules ranges from 0.05 – 0.50  $\mu\text{m}$  (Sudo, 1953), which is a common morphology in weathered volcanic ashes and pumices; Noro, 1986; Tazaki, 1979, 1982; Churchman & Theng, 1984; Nagasawa & Noro, 1987; Ward & cjs, 1990 among others). Spheroidal morphology is related to the saturation state of solutions. Since the dissolution rate of volcanic glass is high, the solution in contact with the glass is likely to be highly supersaturated. By analogy with the formation of spheroidal kaolinite from solution, this condition leads to the precipitation of spheroidal halloysite (Tomura et al., 1985; Huertas et al., 1999).

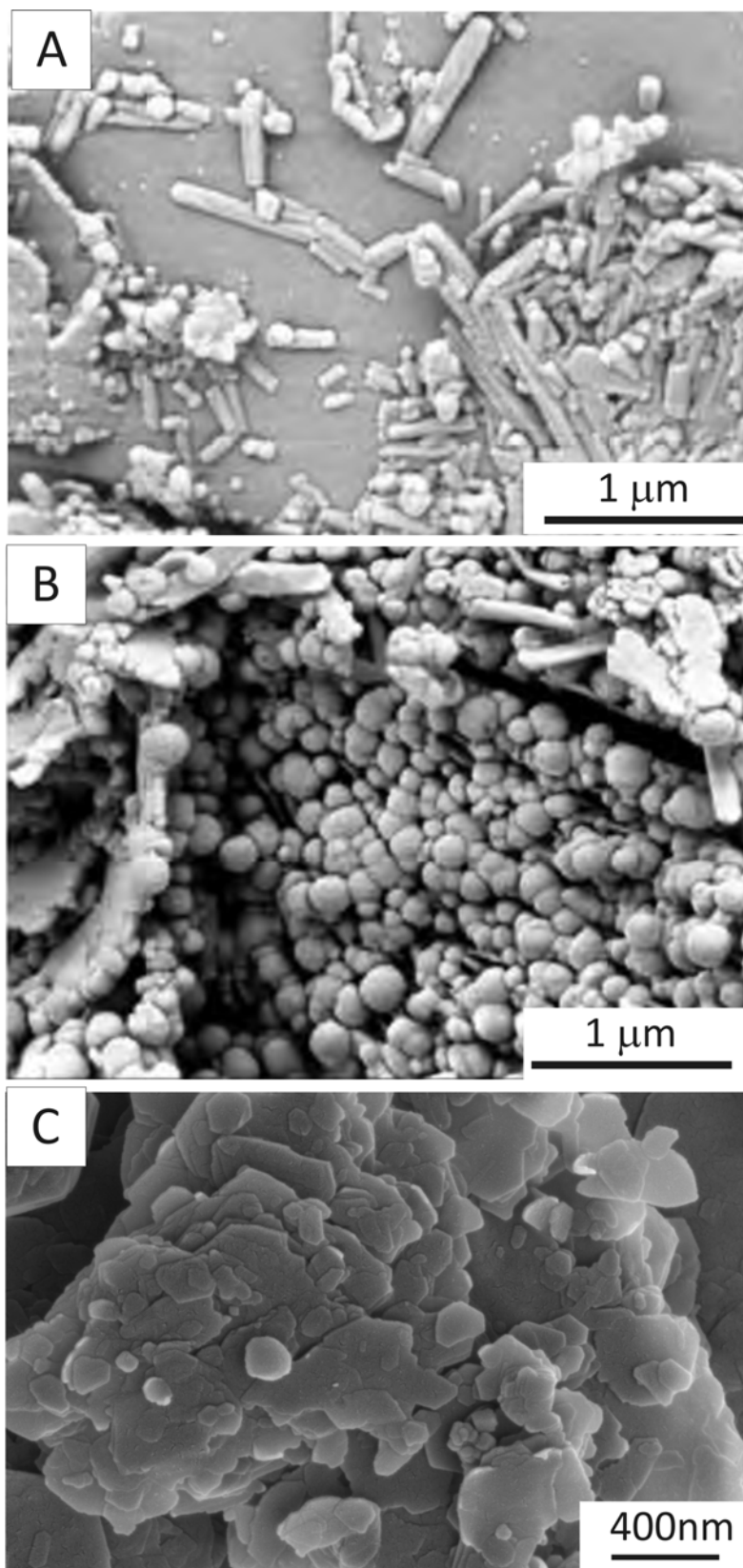


Figure 2: SEM images showing morphologies of halloysite. Short-tube and spheroidal (A, B) and tabular halloysite (C). A, B modified from Ecce & Shroeder, (2007).

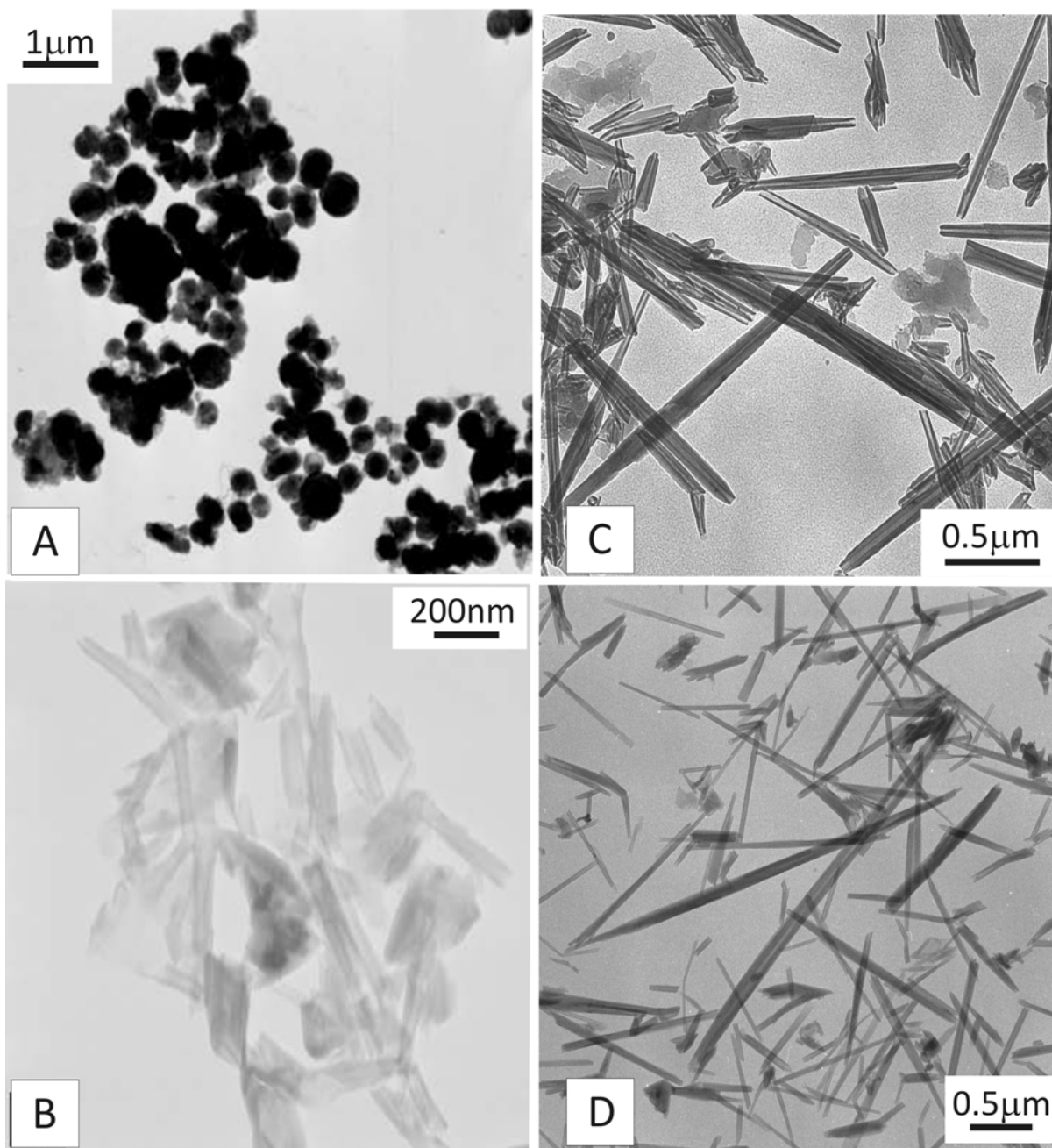


Figure 3: TEM images showing morphologies of halloysite; spheroidal (A), short-tubes (B), and long-tubes (C, D). A, B modified from Joussein et al. (2005), and C, D modified from Inoue et al. (2012).

The dominant morphology of halloysite is tubular. The tubules may be long and thin, short and stubby, or emerging from other tubes (see Nagasawa & Miyazaki, 1976; Noro et al., 1981; Nagasawa & Noro, 1987; Churchman et al., 1995; Adamo et al., 2001). The lengths of halloysite tubules cover a wide range from 0.02 to  $> 30\mu\text{m}$ , whereas their widths range from  $< 0.05$  to  $0.2\mu\text{m}$ . The greater curvature of the core of halloysite crystals seems to be linked to a smaller number of stacked layers (Dixon & McKee, 1974). Most workers have considered curved halloysite tubes to be derived from crystalline minerals such as feldspar and mica. These alteration processes involve the dissolution of previous phases and may involve the formation of an amorphous phase because the structures of these parent minerals are completely different from that of halloysite (e.g. Nagasawa & Noro, 1987). Singh and Silkes (1992) suggest that they are produced by the rolling of platy kaolinite. They show plates fracturing and folding to form tubes. Robertson and Eggleton (1991) used TEM to show the alteration of kaolinite plates to tubular halloysite. More recently, Kogure et al. (2013) have reported, by HRTEM, the occurrence of prismatic halloysite as the consequence of the dehydration of halloysite-(10 Å) to halloysite-(7 Å) and the development of stacking parallel to the (001) layers.

Halloysite plates (or laths) have also been described, but less frequently than tubular or spheroidal halloysites. They are cited in volcanic ash soils, weathered pyroclastic, lateritic profiles, and in felsic plutonic rocks with hydrothermal alteration (Wicke et al., 1978; Carson & Kunzezo, 1970; Wada & Mizota, 1982; Nagasawa & Myazaki, 1976; Noro, 1986; Tazaki, 1979, 1982; De Souza Santos et al., 1965, 1966).

The majority of halloysites are rich in iron in the octahedral layer. The influence of iron contents on particle morphology has been well documented (Churchman, 2000; Hart et al., 2002), and this is probably because the iron content influences the b dimensions of the structure (Radoslovich, 1963; Noro, 1986; Bailey, 1990). Platy forms always contain relatively large amounts of iron (2 – 6% in  $\text{Fe}_2\text{O}_3$ ), whereas tubular particles are relatively Fe-poor (0 – 3%  $\text{Fe}_2\text{O}_3$ ). Spheroidal halloysites exhibit a wide range of iron contents, from almost zero up to values comparable to those of any tubular halloysites (Noro, 1986; Churchman & Theng, 1984; Joussein et al., 2005). A trend is observed within tubular halloysites for the length of tubes to decrease as the structural iron content increases (Churchman & Theng, 1984; Churchman, 2000). Churchman & Theng (1984) suggest that a low concentration of iron in the system at the time of halloysite crystallization tends to favour long tubes; in contrast, appreciable concentrations of iron encourage nucleation, leading to short tubes. The iron content does not appear to influence the formation of spheroidal halloysites strongly. Instead, their formation may be influenced largely by their parent material and its rate of dissolution.

Kaolinites usually show planar morphologies like the other kaolin minerals (nacrite and dickite) (Fig 4). However, some authors have suggested a relationship between the struc-

tural iron and the kaolinite defects. There seems to be a decrease in crystallinity, and possibly in particle size, with an increase in iron substitution (Herbillon et al., 1976; Mestdagh et al., 1980; Mestdagh et al., 1982; Cases et al., 1982). Balan et al. (2007) suggest that the proportion of  $\text{Fe}^{3+}$  ions located near a stacking fault is similar to that occurring in normally stacked layers. This is an indication that the formation of stacking faults in kaolinite is not related to the occurrence of structural  $\text{Fe}^{3+}$  ions as previously observed in other kaolinite samples (e.g. Brindley et al., 1986; Stone and Torres-Sánchez, 1988; Petit and Decarreau, 1990; Balan et al., 2000). More recently, high-resolution TEM research has shown that kaolinite crystals have a high density of stacking defects (Kogure & Inoue, 2005), and that the degree of stacking disorder varies among individual grains (Kogure et al., 2010). Stacking faults are mainly caused by alternating  $t_1$  and  $t_2$  layer displacements and displacement of the octahedral vacancy, and/or by layer rotation. A high density of stacking defects in kaolinite produces lower crystallinity.

In tubular halloysite, the long axis is frequently coincident with the  $b$  axis, and only rarely with the  $a$  axis or another crystallographic direction in the  $a - b$  plan (Kohyama et al., 1978; Anand et al., 1985; Bailey, 1990). The tubes are formed by layer rolling caused by the dimensional misfit between the octahedral and tetrahedral sheets and weak interlayer bonding (Bates et al., 1950; Bates, 1959; Bailey, 1990). In halloysite-10 Å layers, rolling leaves a very small space between two adjacent layers. Although dehydration does not change this arrangement, shrinkage perpendicular to the  $a - b$  plane gives rise to large voids between different parts of the rolls (Kohyama et al., 1978; Churchman et al., 1995). The resulting increase in the overall size of the octahedral layer lessens the dimensional misfit between the octahedral and tetrahedral sheets, allowing the adoption of a planar shape as in kaolinite. The dimensional misfit between the octahedral and tetrahedral sheets also applies to kaolinite, but in this case the misfit is corrected by the rotation of alternate tetrahedrals in opposite directions (Radoslovich, 1963; Bailey, 1990). In halloysite, this rotation is blocked by interlayered water molecules. The basal oxygen atoms of the tetrahedral sheet form a regular six-fold hexagonal structure, producing a 2M1 layer sequence. In kaolinite, on the other hand, the symmetry of the basal oxygens is ditrigonal (distorted hexagonal) with a 1M sequence. According to Singh (1996), the misfit between the apical oxygen plane and the inner OH plane can be corrected by a combination of layer rolling and tetrahedral rotation. The rolling mechanism encounters significantly less resistance from Si-Si repulsion than from tetrahedral rotation. The octahedral sheet probably provides only negligible resistance to rolling.

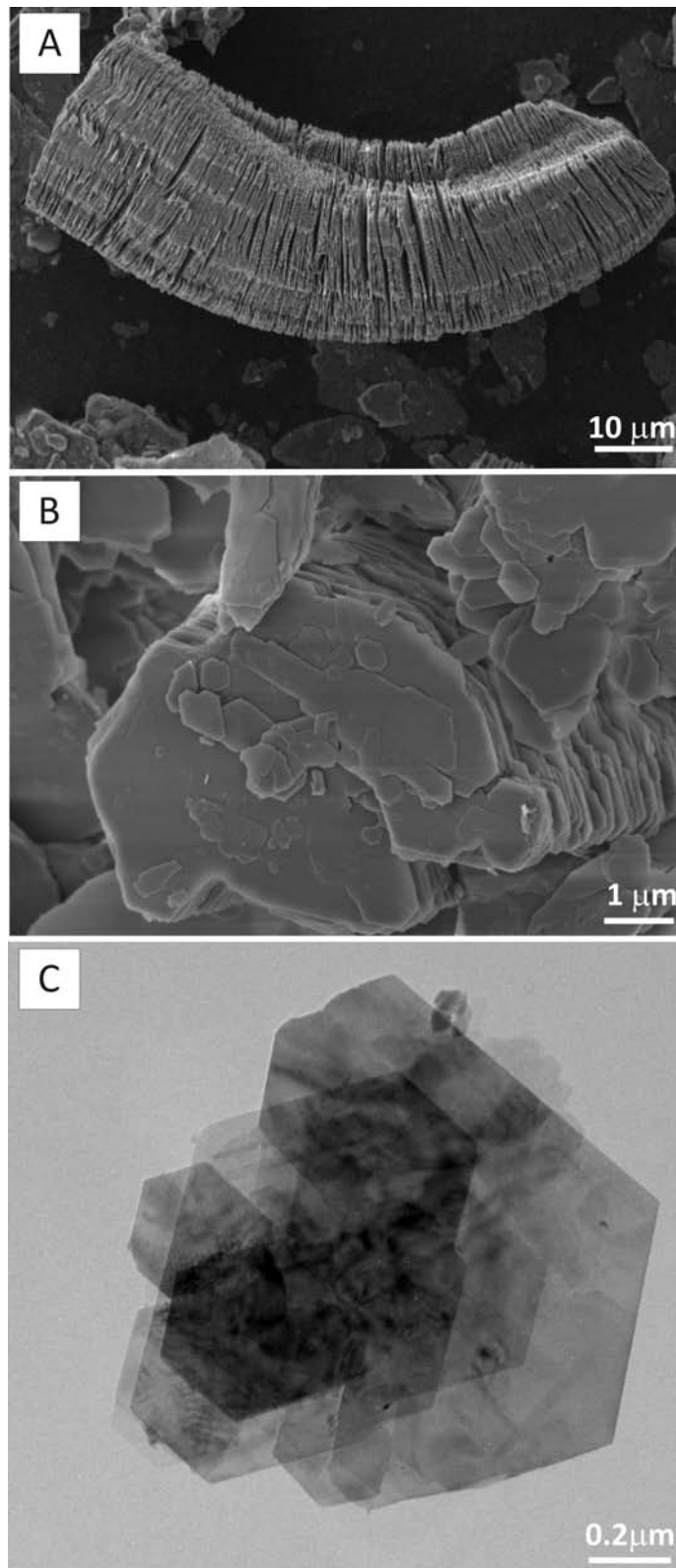


Figure 4: Electron microscope images of a kaolin formed under weathering conditions. SEM images of vermicular aggregates of kaolinites (A) formed by planar and pseudo-hexagonal plates (B). TEM image of single pseudo-hexagonal plates of kaolinite (C).

## 6 Genesis and geological occurrences

Great attention has been paid to the genetic relation between halloysite and kaolinite; however, this relation is difficult to demonstrate because of their structural and chemical similarity. Gorbachev in 1977 already indicated from thermodynamic studies that halloysite is a metastable mineral forming during feldspar alteration and precipitating from aluminium solutions. With enough time, the halloysite may be completely replaced by the more stable kaolinite during the dehydration of halloysite. In nature, it is not easy to establish the condition of formation of these minerals because the kinetics of the mineral reaction at low-temperature environments is controlled by different factors such as temperature, time, the fluid/rock ratio, and the composition of fluids and source rock. As mentioned in the previous section, the relative abundance of halloysite with respect to kaolinite decreases with increasing weathering and hydrothermal alteration. Parham (1969 a,b) suggested that halloysite can be rapidly converted into platy kaolinite. De Souza Santos et al. (1965) reports that drying may alter hydrated tubular halloysite to tubular kaolinite via dehydrated halloysite. The reverse transformation of kaolinite to halloysite was reported by Tari et al. (1999) and Bobos et al. (2001). Singh & Gilkes (1992) explained the transformation in terms of fragmentation into laths that roll to form halloysite (Singh, 1996; Singh & Mackinnon 1996). The reasons why kaolinite becomes hydrated in a natural environment are still unclear.

Halloysite and kaolinite are abundant phases in soils and in weathered and hydrothermally altered rocks.

In soils, halloysite has been described more frequently than kaolinite. In volcanic or ash soils, tubular halloysite crystals with relatively low iron concentrations and platy halloysite crystals with higher iron concentrations have been described by Hart et al. (2002). Dudas and Harward (1975) identify halloysite and some allophane, and Delvaux et al. (1992) describe the coexistence of halloysite and kaolinite in volcanic soils. They suggest a sequence where kaolinite content progressively increases at the expense of hydrated halloysite with increased soil weathering. Accordingly, particle shape varies from spheroids to tubes and then to plates. In soils developed on felsic and metamorphic rocks, the formation of gels and halloysite-like minerals with a great variety of morphologies, planar, spheroidal, and tubular and gels have been described from the alteration of feldspars and phyllosilicates (Romero et al., 1992). These authors suggest that the formation of an intermediate amorphous phase promotes halloysite crystallization.

In weathered rocks, halloysite and kaolinite can form from primary minerals. In all cases, there is a dissolution process of primary minerals (feldspars, muscovite, and biotite) and crystallization of the kaolin minerals. The process is more effective under humid and temperate climates. Jeong et al. (2000) describe, in a weathering profile of granite, how

the plagioclase is partially weathered to halloysite and biotite to kaolinite via the crystallization of mixed-layer biotite/vermiculite. The formation of halloysite or kaolinite in this case is controlled by the structure of the primary rock. Samotoin & Bortnikov (2011) describe the replacement of muscovite, biotite, and chlorite by kaolinite in granites and pegmatites. The kaolinite is formed from a solution that arises owing to the decomposition of primary minerals and crystallizes immediately at the surface of these minerals without the participation of any intermediate amorphous or crystalline phases. They describe several stages: formation of solutions related to decomposition of primary minerals, growth of kaolinite layers in epitactic orientation on (001) surfaces of primary minerals, formation of steps of screw dislocations at the surface of kaolinite nanocrystals, growth controlled by a helical mechanism, and finally, the formation of pseudomorphs replacing primary minerals. Inoue et al. (2012) show the crystallization of tubular halloysite via the dissolution of feldspars in a quartzdiorite and precipitation from solution. When the fluid/rock ratio decreases, the halloysite begins to dehydrate and dissolve. Nucleation of kaolinite takes place on the edges and in the shrinkage pores of dehydrated halloysite. At the incipient growing stages of kaolinite, there is a topotactic relationship of  $b^*$  halloysite parallel to  $b^*$  kaolinite. Robertson and Eggleton (1991) describe, by SEM and TEM, the alteration process of muscovite to kaolinite and, subsequently, from kaolinite to halloysite. The growth of kaolinite from muscovite has a topotactic relation with (001) parallel layers in both minerals. Galán & Vivaldi (1973) describe the formation of kaolinite and minor halloysite and allophone from feldspars and micas by the weathering of felsic igneous rocks. Singh and Silkes (1992) suggest the alteration of mica to kaolinite and kaolinite to halloysite by the rolling of platy kaolinite. They show plates of kaolinite fracturing and folding to form tubes. Magasawa & Noro (1987) indicate that the weathering of feldspar in granitic rocks produces tubular halloysite; in contrast, the weathering product of pyroclastic/vitreous materials takes the shape of balls, nodules, scrolls, or short tubes. Hong et al. (2009) describe the crystallization of halloysite from a Si-Al amorphous gel in a laterite profile, along with the dissolution of coarse-grained kaolinite ( $1 - 2 \mu\text{m}$ ) with irregular or rounded edges, uneven (001) surfaces, and well-developed amorphous spots in kaolinite crystals. All of these features evidence dissolution of the previous coarser kaolinite particles, and Bauluz et al. (2008) report the crystallization of nanoparticles of kaolinite from the alteration of K-feldspar via the formation of an Al-Si gel. In sedimentary rocks and paleosoils, kaolinite can be a very abundant clay mineral. In contrast, in these lithologies halloysite is usually scarce. Kaolinite formation requires intensive weathering involving warm to tropical temperatures and high rates of fresh water percolation through feldspar and other minerals in source rocks (Weaver, 1989; Robert and Kennett, 1992). An increase in the rate of water percolation through a source rock of requisite composition under warm conditions usually results in an increase in the

amount of kaolinite formed. There are some geological periods whose record contains abundant kaolinite, and they have been associated to warm, humid climate conditions such the Lower Cretaceous and the Paleocene–Eocene boundary (Fig. 5).

During the Lower Cretaceous (Wealden), a warm, humid regime has been documented through northwest Europe (Wright et al., 2000) and southwest Europe (Bauluz et al., 2014, 2015). From studies in southern England, the Wealden climate was summarized by Allen (1998) as seasonal in nature and hot to very warm (circa 25°C), alternating with cooler periods (circa 10°C). They describe periods of high rainfall alternating with remissions and droughts. Haywood et al. (2004) reports a paleoclimate model for the Early Cretaceous (Barremian) focusing on the Weald of SE England. The model predicts cold months (4 – 8°C) and warm months (36 – 40°C) with high precipitation rates for all seasons with little evidence for prolonged drought.

Wright et al. (2000) describe facies and mineralogical evidence of the development of paleosoils formed during warm, humid conditions in non-marine sections in southern England. Bauluz et al. (2010a, 2011, 2012, 2014, 2015) report the occurrence of abundant kaolinite in continental siliciclastic series (Barremian) in the Iberian Range (NE Spain) (Fig. 6). The textural and crystallochemical characteristics of the kaolinites (inferred from XRD, SEM, and TEM) support an authigenic origin related to paleoclimate conditions. The availability of rainfall promoted dissolution silicates (quartz and feldspars) and the crystallization of kaolinite replacing these silicates and filling sediment pores.

During the Weald, bauxites and iron-rich paleosoils formed in Europe (Bardossy, 1982; Molina & Salas, 1993; Yuste et al., 2014). The term bauxite is used for lithified or unlithified residual weathering products rich in alumina and low in alkali elements, alkaline earth, and silica (Gow & Linozej, 1993). Bauxite occurs in a variety of textural forms, ranging from earthy through pisolitic to structured or massive. Mineralogically, they consist mainly of a mixture of Al hydroxides (gibbsite, diaspore, and boehmite), kaolinite, and Fe and Ti oxides and hydroxides. Bauxites described by Yuste et al. (2014) in the Iberian Range (NE Spain) are karst bauxites and belong to the Mediterranean-type karst bauxites of Bardossy (1982). These bauxites have complex pisolitic structures and are composed of well-crystallized kaolinite, gibbsite, goethite, and hematites (Fig. 7). SEM and XRD observations suggest that the bauxitization process took place in several stages, implying variations in water saturation conditions and coetaneity with intense weathering even during the Lower Cretaceous.

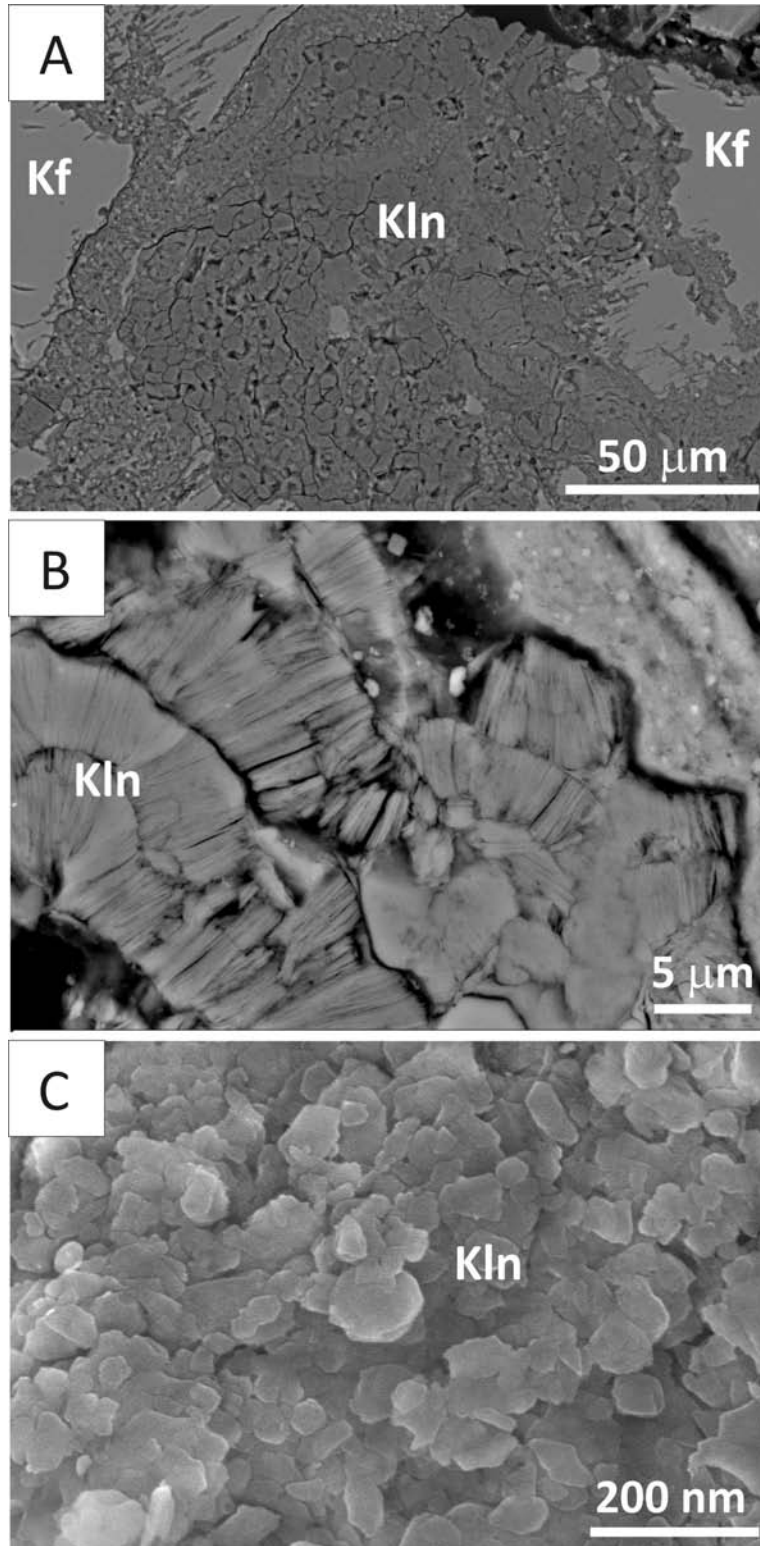


Figure 5: SEM images of a Paleocene–Eocene paleosol from NE Argentina. (A) Altered K feldspar that is replaced by kaolinite. Large magnification of kaolinite forming aggregates (B) and single particles of kaolinite forming the matrix (C). Kln= kaolinite, Kf= K feldspar.

An abrupt climate warming of 5 – 10°C during the Paleocene–Eocene boundary thermal maximum (PETM) 55 Myr ago is linked to the catastrophic release of  $\sim 1,050$ – $2,100$  Gt of carbon from seafloor methane hydrate reservoirs (Dickens et al., 1997). Although this methane and the CO<sub>2</sub> derived from oxidation probably contributed to the PETM warming, there is evidence based on carbon-isotope records that indicates a shift in the state of the climate during this period, characterized by large increases in mid-latitude tropospheric humidity and enhanced carbon cycling through terrestrial ecosystems (Bowen et al., 2004). This relative warming also produced a signal in the clay mineralogy associations promoting the crystallization of kaolinite. However, there are still some unresolved questions.

In marine sediments, Gibson et al. (2000) describe kaolinite-dominated clay suites in the latest Paleocene in the northern US Atlantic Coastal Plain. Kaolinite contents jump from < 5% to 50 – 60%, suggesting to them that kaolinite-rich source areas were widespread in the northeastern US during the latest Paleocene. Erosion of these source areas contributed the kaolinite, which was transported and widely dispersed into shelf environments of the Salisbury embayment. The increase in kaolinite, which occurred during a time of relatively high sea level, is probably the result of intensified weathering due to increased temperature and precipitation. Similar observations are reported by Schneider & Bowen (2013), who describe changes in inorganic nitrogen burial, clay minerals, and clastic grain size in near-shore marine sediments in New Jersey (USA) throughout the PETM, associated with enhanced continental weathering, erosion, and redeposition of ancient kaolinites, and eustatic sea-level variations. Bolle and Adatte (2001) studied Tethys (Egypt, Israel, Tunisia, Spain, and Kazakhstan) and Atlantic (England) marine sections, reporting a widespread abundance of kaolinite in marine sediments at all locations, which suggests a warm, humid climate with high rainfall during the late PETM. However, in coastal basins along the southern margin, warm, arid conditions associated with enhanced evaporation continued. In several papers focusing on the Paleocene–Eocene boundary in Williston Basin (North Dakota), they describe a terrestrial weathering profile characterized by intense pedogenesis during an ancient (circa 55 Ma) global event. The profile contains abundant kaolinite, poor organic carbon preservation, and ferric pisoliths. Handley et al. (2011) have suggested that the humid climate often suggested for the PETM was not global in nature.

Halloysite and kaolinite can also form by hydrothermal alteration. They are alteration products of dissolution/crystallization processes associated with moderately acid hydrothermal solutions. Previously, the primary phases in the rock (feldspars, phyllosilicates, volcanic glass, etc.) are dissolved by the solutions and, subsequently, the crystallization of halloysite and kaolinite takes place. The process depends on the temperature and composition of the hydrothermal fluid, rock/fluid ratio, and the composition of the primary rock. Therefore, the temperature crystallization of halloysite and kaolinite may

be variable. In general, halloysite crystallizes at temperatures below 100°C, kaolinite crystallizes at temperatures between 100 and 270°C, and pyrophyllite can form at temperatures higher than 270°C (Inoue, 1995; Bauluz & Subías, 2010). In their review of Spanish kaolin deposits, Galán & Vivaldi (1973) refer to the difficulty of distinguishing hydrothermal from weathered kaolin when alteration temperatures are very low. The formation of halloysite and kaolinite has been described by the hydrothermal alteration of different types of felsic rocks (volcanic and plutonic igneous rocks, and sedimentary rocks). These authors describe the formation of kaolinite and variable proportions of halloysite from hydrothermally altered felsic plutonic and metamorphic rocks that form large deposits in NW Spain. Ecce and Shroeder (2007) report the formation of halloysite (7 Å and 10 Å) and alunite from the hydrothermal alteration of volcanic rocks. Domínguez et al. (2010) show the alteration of subalkaline rhyolites that produces the crystallization of both kaolinite and halloysite; they establish at least three kaolinite generations during the alteration. Bauluz et al. (2010b) report the crystallization of kaolinite from ignimbrites in a silver epithermal deposit.

Ece et al. (2013) report the crystallization of halloysite and kaolinite in a hydrothermal system in volcanic rocks at temperatures of 38 – 129°C. From the alteration of felsic intrusive rocks, Muhammad & Zulfiqar (2008) describe kaolinite crystallization. In siliclastic rocks, Drews-Arnitage et al. (1996) report both the formation of kaolinite and halloysite. Kaolinite crystallization is associated to hydrothermal alteration with temperatures higher than 75°C and halloysite is associated to supergene alteration at lower temperatures and a higher pH than kaolinite formation.

## 7 Technological applications

### *Kaolin applications*

Kaolins are rocks comprised largely of one of the kaolin group of minerals (kaolinite, halloysite, dickite, and nacrite), and they can form both by weathering and hydrothermal alteration processes. The properties and applications of kaolinite (the most common kaolin mineral) are considered in this section. Kaolinite and kaolins have many industrial uses (Murray, 1963, 1999; Konta, 1980, 1995; González-López, 2000; King, 2009, among others), so only a brief summary of their applications is given. Kaolinite uses derive from favourable properties such as natural whiteness, fine particle size, non-abrasiveness, and chemical stability. Kaolinite is soft, has a low viscosity at high solids content in many systems, is readily wetted and dispersed in water and some organic systems, and can be produced with a controlled particle size distribution.

More than 50% of kaolin production is for the paper industry. Kaolin is used as a filler in the interstices of the sheet, which adds ink receptivity and opacity to the paper sheet.

Kaolin coating on the surface of the paper sheet makes sharp photographic illustrations and bright printed colours possible. The significant properties of kaolin of greatest value to the paper industry are whiteness, low viscosity, non-abrasiveness, controlled particle sizes, and flat hexagonal plates. Opacity, in particular, is an extremely important property to the paper industry. Brightness, gloss, and viscosity properties also depend on particle size (Lyons, 1958). Flow properties of kaolin clays, especially the kaolin coating clays used in the paper industry, are very important because of their influence on coat weight, smoothness, texture, and other properties. The rheology of kaolin is affected by particle size distribution, particle shape, electrokinetic effects between particles, the presence of impurities, and the degree of flocculation and dispersion.

Kaolin is used as a filler in many rubber goods. It adds strength, abrasion resistance, and rigidity to both natural and synthetic rubber products. In general, most rubber products extrude more easily after a kaolin filler is added. The primary reason that kaolin is used in rubber compounds is its whiteness and low cost, but it has excellent functional properties despite costing less than most other rubber pigments.

Kaolin is used in ceramic white ware products, insulators, and refractories in white wares. It aids in accurate control of moulding properties and adds dry and fired strength, dimensional stability, and a smooth surface finish to the ware. The excellent dielectric properties and chemical inertness of kaolin make it well suited for porcelain electrical insulators. In refractory applications, its dimensional stability, low water content, and high green strength make kaolin an important component.

Kaolin is used in paint because it is chemically inert, insoluble in the paint system, has a high covering power, gives the paint desirable flow properties, and is low in cost.

The addition of kaolin to thermosetting and thermoplastic mixes gives smoother surfaces, a more attractive finish, good dimensional stability, and high resistance to chemical attack. In addition, the flat hexagonal kaolin plates hide the reinforcing fibres and give the mix flow ability to simplify tile moulding of complex shapes.

Another special application for kaolinite is in the production of synthetic zeolites. Kaolinite can be treated with Na, Ca, Mg, and K hydroxides which, when heated to  $\sim 100^\circ\text{C}$ , will convert the kaolinite to zeolite structures with different pore sizes. These synthetic zeolites are used primarily as cracking catalysts in petroleum refining and to remove water from gas streams.

Kaolin has many other industrial applications for manufacturing ink, cement, detergents, adhesives, fertilizers, porcelain, enamels, insecticides, plaster, medicines, roofing granules, food additives, cosmetics, catalysts, chemicals, textiles, and so on.

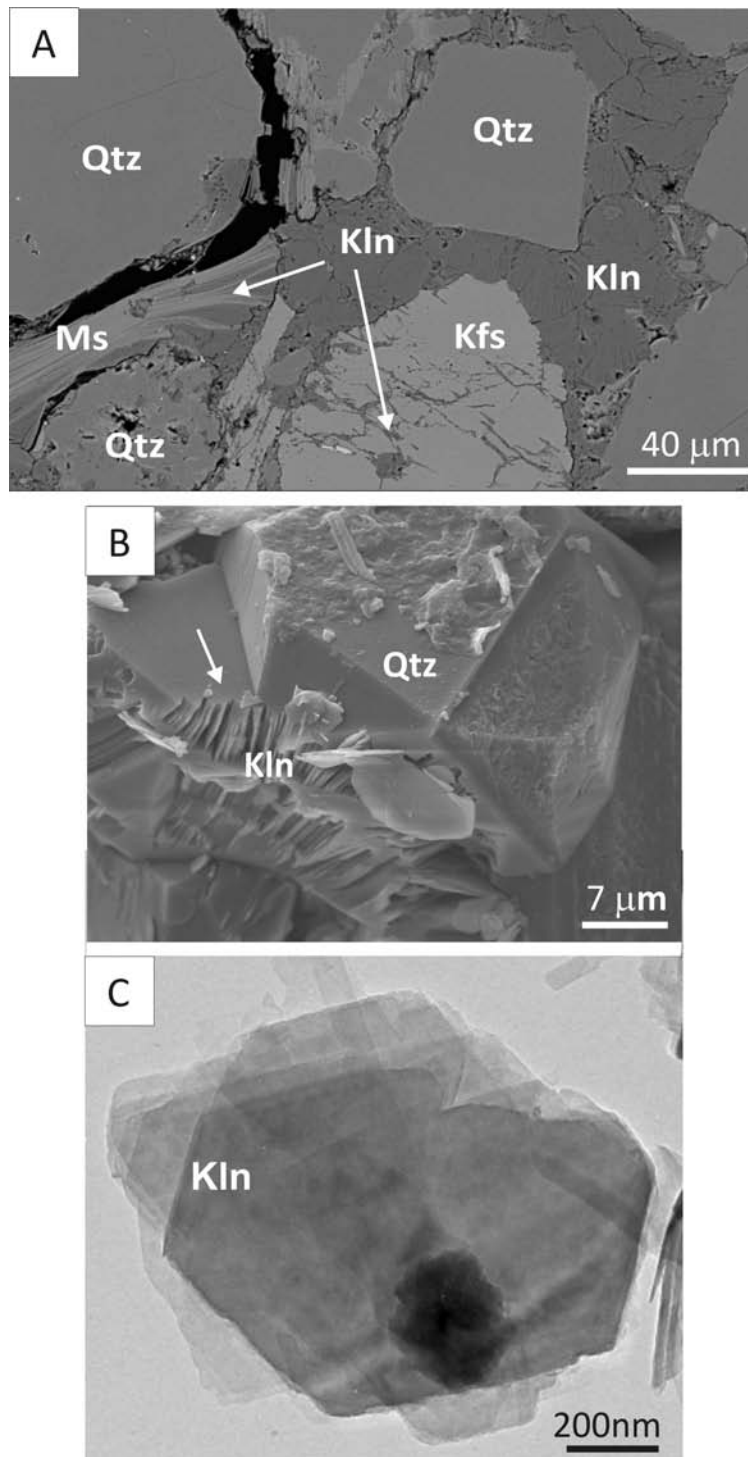


Figure 6: Electron Microscopy images of the Lower Cretaceous from the SE Iberian Range. A) SEM image of the texture of the rock. The image shows the replacement of K feldspars to kaolinite and the growth of kaolinite between the muscovite (Ms) cleavages. B) SEM images of quartz being replaced by kaolinite, C) TEM image of single crystals of kaolinite. Images modified from Bauluz et al. (2014). Kln= kaolinite, Qtz= quartz, Ms= muscovite, Kfs= K feldspar.

### *Halloysite applications*

As Kamble et al. (2012) suggest, in the field of pharmacy and health care, effectiveness of medicine and therapy is very important, failure or drawback in the drug therapy may lead to either ineffectiveness or side effects that hamper human health. Green nanotechnology aims at developing environmentally safe and less harmful nanoproducts. Halloysite clay nanotubes, nanocomposites, nanopowders, and so on are now emerging as trendsetters in green nanotechnology. Halloysite nanotubes (HNs) are ecofriendly nanotubes with a lower cost than carbon nanotubes. In recent years, there has been growing concern about the effect of carbon nanotubes on human health and on the environment because of their potentially toxic nature. HNs have numerous commercial applications including as additives in polymers and plastic, electronic components, drug delivery vehicles, cosmetics, and in home and personal care products.

Halloysite uses derive from its favourable properties (Schaefer, 2008; Mingliang et al., 2010) as a natural, nontoxic, and biocompatible mineral with a fine particle size, high surface area, superb dispersion, and high cation exchange capacity. It maintains uniform, sustained release rates and no initial overdosage. Halloysite is capable of prohibiting release unless triggered, thus providing tuneable release rates, and it is capable of loading multiple active agents simultaneously (Kamble et al., 2012). Halloysite reduces the volume of costly active agents, is implementable in many forms such as powders, creams, gels, lotions, and sprays. It has superior loading rates compared to other carriers, a fast adsorption rate and high adsorption capacity, in addition to high porosity and non-swelling. HNs are used for capturing circulating tumour cells. It was found that halloysite nanotube coatings promote an increased capture of leukemic cells; the key parameters that control cell capture under flow are the halloysite content and selection density (Hughes & King, 2010). HNs have also been investigated as a tubular container for the corrosion inhibitor benzotriazole, and as an additive in paints to produce a functional composite coating material (Dmitry et al., 2008).

HNs may be applied for controlled release. By varying internal fluid properties, the formation of nanoshells over the nanotubes, and of smart caps at the tube ends it is possible to develop various means of controlling the rate of release. They can also be used as protective coatings for the loading of agents for metal and plastic anticorrosion protection (Price et al., 2001). HNs are capable of entrapping active agents within the core lumen and in any void spaces contained in the multilayered walls of the cylinder. Halloysite is capable of retaining and releasing both hydrophilic and hydrophobic agents. HNs can be applied as a special delivery system. They are combined with existing pharmaceuticals for sustained drug delivery. Compared to carbon nanotubes, HNs are less expensive and have a larger surface area, which allows for greater control of drug loading

and elution profiles ([www.nanoclay.com](http://www.nanoclay.com)). As an example, HNs can carrier ZnO, which is an antimicrobial agent, into the lumen and surface, which produces an active packaging film where ZnO can strongly influence the antimicrobial activity of the HNs (Pasbakhsh & Churchman, 2015).

HNs may also be applied in wound-care products, promoting healing and reducing the chances of infection and scarring. Using halloysite as a drug delivery system in cases of burn care can be very beneficial. They are natural nanocontainers for the controlled delivery of glycerol as a moisturizing agent for the loading and extended release of glycerol for cosmetic applications (Dmitry et al., 2008), and they can be applied as a skin cleanser without an active agent (Cao et al., 2009).

HNs can also be applied as nano-sorbents for contaminants and pollutants from aqueous solutions (Liu et al., 2009).

## 8 Conclusions

Kaolinite and halloysite have a similar structure, composition, and genesis. Both minerals are dioctahedral 1:1 layer silicates and, compositionally, hydrated aluminium silicates. Halloysite and kaolinite may occur together in nature because they form under similar conditions in soils and in weathered and hydrothermal rock alterations. Their structure, morphologies, and physical properties make them useful for technological applications. More research on applying new techniques may increase our knowledge of their structure and genesis, and this knowledge will be useful in improving the processing and development of new applications.

## Acknowledgments

The author is very grateful to Prof. Juan Jiménez-Millán (University of Jaen) for his constructive comments and to Christine Laurin for English editing. The author is extremely grateful to Prof. José Manuel González López (University of Zaragoza), Prof. Donald R. Peacor (University of Michigan), and Prof. Fernando Nieto (University of Granada) for introducing her to the study of clays and the electron microscopy. The author also wants to thank Dr. María José Mayayo, Dr. Alfonso Yuste, and Dr. Ignacio Subías, members of her research group (*Recursos Minerales*, University of Zaragoza) for their collaboration during these years. Financial support for the research on clay development by the author and cited in this paper was provided by Research Projects CGL2009-07574 and CGL2013-46169-C2-1-P (Spanish Ministry of Science and Technology) and the Gobierno de Aragón and the European Social Fund (*Grupos consolidados*).

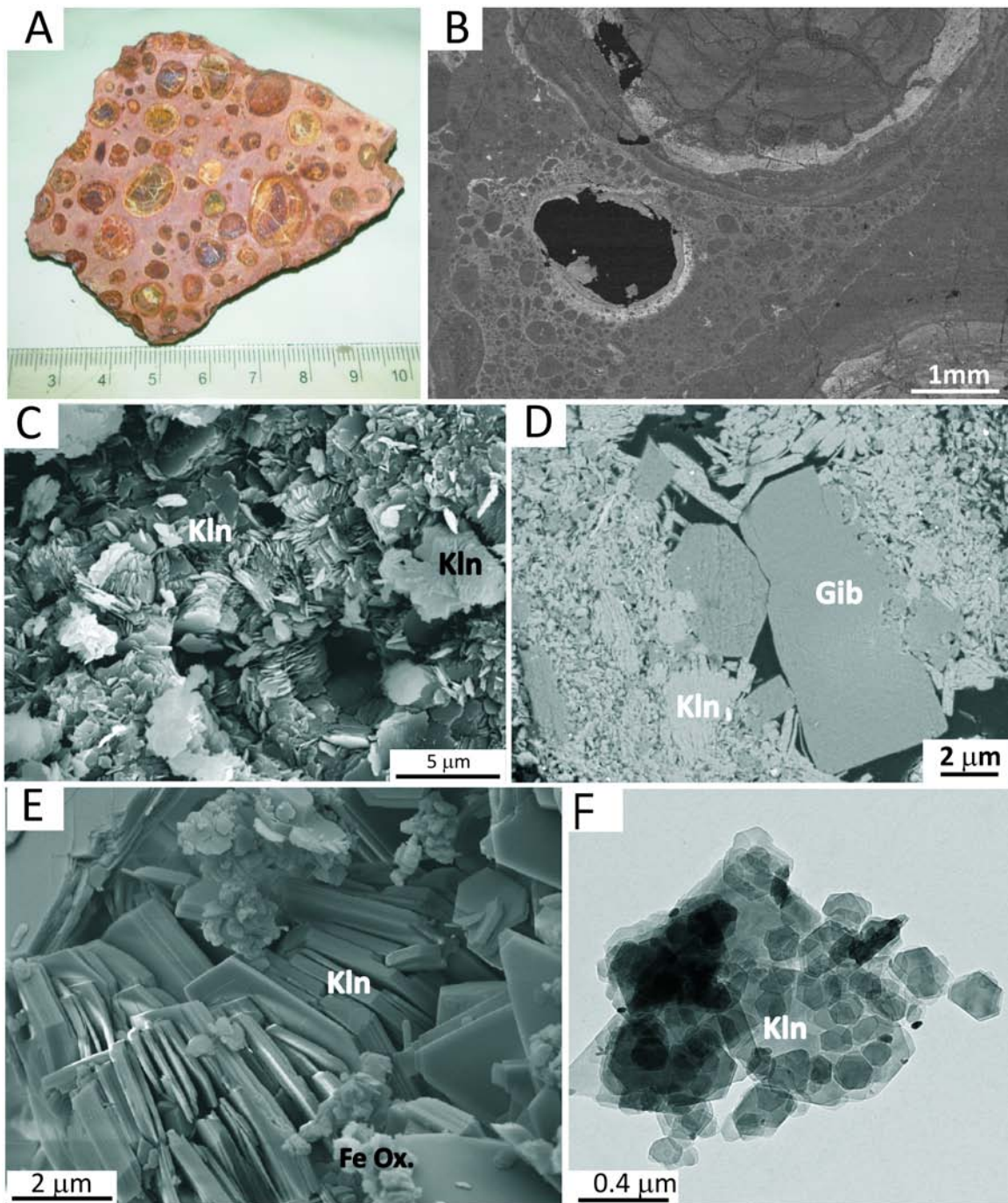


Figure 7: Images corresponding to bauxites of the SE Iberian Range. Hand sample of a bauxite fragment with its characteristic pisolithic texture (A). SEM images showing the pisolithic texture (B), kaolinite plates forming the matrix (C), the replacement of gibbsite by kaolinite (D) and kaolinite booklets forming the pisolites and matrix of the rock (E). TEM image of single particles of kaolinite (F). B, C and D modified from Yuste et al. (2014). Kln= kaolinite, Gbs= gibbsite, Fe Ox= Fe oxides.

## 9 References

- Adamo P., Violante P. & Wilson M.J. (2001): Tubular and spheroidal halloysite in pyroclastic deposits in the area of the Roccamonfina volcano (southern Italy). *Geoderma*, 99, 295–316.
- Allen P. (1998): Purbeck-Wealden (early Cretaceous) climates. *Proc. Geologist's Association*, 109, 197–236.
- Anand R.R., Gilkes R.J., Armitage T.M. & Hillyer J.W. (1985): Feldspar weathering in a lateritic saprolite. *Clays Clay Minerals*, 33, 31–43.
- Bailey S.W. (1990): Halloysite – A critical assessment. Pp. 89–98 in: *Surface Chemistry Structure and Mixed Layering of Clays*. Proceedings of the 9<sup>th</sup> Int. Clay Conf. 1989 (V.C. Farmer & Y. Tardy, eds.). *Sciences Géologiques, Memoire*, 86, Strasbourg, France.
- Bailey, S.W. (1988): Polytypism of 1:1 layer silicates. In *Hydrous Phyllosilicates (Exclusive of Micas)*, S.W. Bailey (ed.), pp. 9–27. *Reviews in Mineralogy*, Min. Soc. America, Chantilly, Virginia.
- Balan, E., Allard, T., Boizot, B., Morin, G. & Muller, J.P. (2000): Concentration of paramagnetic structural Fe<sup>3+</sup> in natural kaolinites. *Clays Clay Minerals*, 48, 439–445.
- Balan, E., Fritsch, E.M. Allard, T. & Calas, G. (2007): Inheritance vs. neoformation of kaolinite during lateritic soil formation: A case study in the Amazon basin. *Clays Clay Minerals*, 55, 253–259.
- Bardossy, G. (1982): *Karst Bauxites. Bauxite Deposits on Carbonate Rocks*. Elsevier, Amsterdam.
- Bates, T.F. (1959): Morphology and crystal chemistry of 1:1 layer lattice silicates. *Am. Miner.*, 44, 78–114.
- Bates, T.F., Hildebrand, F.A. & Swineford, A. (1950): Morphology and structure of endellite and halloysite. *Am. Miner.*, 35, 463–484.
- Bauluz, B. (2007): Illitization processes: Series of dioctahedral clays and mechanisms of formation. In: *Diagenesis and Low-Temperature Metamorphism. Theory, Methods and Regional Aspects*. Nieto F. & Jiménez-Millán J. (eds.). *Seminarios SEM*, 3, 31–39, ISSN 1698-5478.
- Bauluz, B. (2013): Clays in low-temperature environments. In: *Minerals at the nanoscale*. Nieto F. & Livi F.T. (eds.). *EMU notes in Mineralogy*, 14, 181–209. Published by the EMU.
- Bauluz, B. & Subías, I. (2010): Coexistence of pyrophyllite, I/S R1, and NH<sub>4</sub><sup>+</sup>-rich illite in Silurian black shales (Sierra de Albarracín, NE Spain): Metamorphic vs. hydrothermal origin. *Clay Min.*, 45, 383–392.
- Bauluz, B., Yuste, A., Mayayo, M.J., González López, J.M. (2008): Kaolinite crystallization from an amorphous phase in diagenetic sandstones. *Reunión SEM-SEA 2008, Macla*, 9, 49–50.
- Bauluz, B., Cedillo, A., Mayayo, M.J., Yuste, A. & González López, J.M. (2010a): Clay mineralogy of the kaolin-rich sedimentary deposits from the Weald facies in the Iberian Range (NE Spain). *18<sup>th</sup> Int. Sediment. Congress. Sedimentology at the foot of the Andes*, p 322.
- Bauluz, B., Cedillo, A. Subías, I., Páez, G., Ruiz, R. & Guido D. (2010b): Hydrothermal clays at

- the Futuro vein, Martha mine silver epithermal deposit, Deseado Massif, Patagonia, Argentina. SEA-CSSJ-CMS Trilateral Meeting on Clay, 117–118. Hermosin, M.C, Celis, R., Undabeytia, T., Bruna F. & Aparicio P. (eds.), Sevilla (Spain).
- Bauluz, B., Yuste, A., Mayayo, M.J. & González López, J.M. (2011): Very early kaolinization of Weald facies sedimentary deposits in the Iberian Range (NE Spain): Possible origin related to a climatic weathering event. Euroclay 2011. Book of Abstracts, p.45.
- Bauluz, B., Yuste, A., Mayayo, M.J. & González López, J.M. (2012): Minerales del caolín en el Weald de la Cubeta de Aliaga (NE España). Distribución e implicaciones geológicas. XXII Reunión Científica de la SEM-XXII Reunión Científica de la SEA. Macla, 16, 92–93.
- Bauluz, B., Yuste, A., Mayayo, M.J. & Canudo, J.I. (2014): Early kaolinization of detrital Weald facies in the Galve Sub-basin (Central Iberian Chain, north-east Spain) and its relationship to palaeoclimate. *Cretaceous Research*. DOI: 10.1016/j.cretres.2014.03.014
- Bauluz, B., Yuste, A., Mayayo, M.J. (2015): The use of the clay mineralogy as a paleoclimate tool: An example of the kaolinite rich-Weald facies in the Iberian Chains (NE Spain). Euroclay 2015. Abstracts Euroclay, p. 366.
- Bobos, I., Duplay J., Rocha J. & Gomes C. (2001): Kaolinite to halloysite-7 Å transformation in the kaolin deposit of Sao Vicente de Pereira, Portugal. *Clays Clay Minerals*, 49, 596–607.
- Bolle, M.P. & Adatte T. (2001): Palaeocene–early Eocene climatic evolution in the Tethyan realm: Clay mineral evidence. *Clay Min*, 36, 249–261.
- Bonnin, D., Muller, S. & Callas, G. (1982): Le fer dans les kaolins. Etude par spectrometries R.P.E., Mosbauer, EXAFS. *Bull. Mineral.*, 105, 467–475.
- Bookin, A.S., Drits, V.A., Plancon, A. & Tchoubar, C. (1989): Stacking faults in kaolin-group minerals in the light of real structural features. *Clays Clay Minerals*, 37, 297–307.
- Bowen, G., Beerling, D.J. & Koch, P.L. (2004): A humid climate state during the Palaeocene/Eocene thermal maximum. *Nature*, 432, 495–499.
- Brindley, G.W. (1980): Order-disorder in the clay mineral structures. Pp. 125–196 in: *Crystal structures of clay minerals and their x-ray identification* (G.W. Brindley & G. Brown, eds.). Mineralogical Society, London.
- Brindley, G.W. & Robinson, K. (1945): Structure of kaolinite. *Nature*, 156, 661–663.
- Brindley, G.W. & Robinson, K. (1946): The structure of kaolinite. *Mineralog. Mag.* 27, 242–253.
- Brindley G.W. & Goodyear J. (1948): X-ray studies of halloysite and metahalloysite. The transition of halloysite to metahalloysite in relation to relative humidity. *Min. Mag.*, 28, 407–422.
- Brindley G.W., Kao C., Harrison J.L., Lipsicas, M. & Raythatha, R. (1986): Relation between structural disorder and other characteristics of kaolinites and dickites. *Clays Clay Minerals*, 34, 239–249.
- Cao, J., Hu, X. & Jiang, D. (2009): Synthesis of Gold Nanoparticle Using Halloysites. *E-Jour. Surf. Sci. Nanotech.*, 7, 813–815.
- Carson, C.D. & Kunzezo, G.W. (1970): New occurrences of tabular halloysite. *Soil Sci. Soc. Am. Proc.*, 34, 538–540.
- Cases, J.M., Lietard, O., Yvon, J. & Delon, J.F. (1982): Études des propriétés cristallographiques,

- morphologiques superficielles de kaolinites désordonnées. *Bull. Min.*, 105, 439–455.
- Chukhrov, F.V. & Zvyagin, B.B. (1966): Halloysite, a crystallochemically and mineralogically distinct species. *Proceedings of the International Clay Conference, 1966* (L. Heller & A. Weiss, eds). Israel Program for Scientific Translation, Jerusalem, Israel.
- Churchman, G.J. (2000): The alteration and formation of soil minerals by weathering. F3-F76 in: *Handbook of Soil Science* (M.E. Sumner, editor). CRC Press, Boca Raton, Florida.
- Churchman G.J. & Theng B.K.G. (1984): Interactions of halloysites with amides: Mineralogical factors affecting complex formation. *Clay Minerals*, 19, 161–175.
- Churchman G.J., Davy T.J., Aylmore L.A.G., Gilkes R.J. & Self P.G. (1995): Characteristics of fine pores in some halloysites. *Clay Minerals*, 30, 89–98.
- de Souza Santos P., Brindley G.W. & de Souza Santos H. (1965): Mineralogical studies of kaolinite-halloysite clays: Part III. A fibrous kaolin mineral from Piedade, Sao Paulo, Brazil. *American Mineralogist*, 50, 619–628.
- de Souza Santos P., de Souza Santos H. & Brindley G.W. (1966): Mineralogical studies of kaolinite-halloysite clays: Part IV. A platy mineral with structural swelling and shrinking characteristics. *American Mineralogist*, 51, 1640–1648.
- Delvaux B., Tessier D., Herbillon A.J., Burtin G., Jaunet A.M. & Vielvoye L. (1992): Morphology, texture, and microstructure of halloysitic soil clays as related to weathering and exchangeable cations. *Clays and Clay Minerals*, 40, 446–456.
- Dickens, G.R., Castillo, M.M. Walker, J.C.G. (1997): A blast gas in the latest Paleocene: Simulating first-order effects of massive dissociation of oceanic methane hydrate. *Geology*, 25, 259–262.
- Dixon, J.B. & McKee, T.R. (1974): Internal and external morphology of tubular and spheroidal halloysite particules. *Clays Clay Minerals*, 22, 127–137.
- Dmitry, G.S., Zheludkevich, M., Yasakau, K., Lamaka, S., Möhwald, H. & Ferreira, M.G.S. (2006): Nanocontainers for Self-Healing Corrosion Protection, *Adv. Mater.*, 18, 1672–1678.
- Domínguez, E., Iglesias, C., Dondi, M. & Murray, H. (2010): Genesis of the La Espingarda kaolin deposit in Patagonia. *App. Clay Sci.*, 47, 290–302.
- Drews-Armitage, S.P., Romberger, S.B. & Whitney, C.G. (1996): Clay alteration and gold deposition in the genesis and blue star deposits, Eureka County, Nevada. *Econ. Geol.*, 91, 1383–1393.
- Dudas, M.J. & Harward, M.E. (1975): Weathering and authigenic halloysite in soil developed in Mazama ash. *Soil Sci. Soc. Amer. Jour.*, 39, 561–566.
- Ece, O. Ekinçi, B., Schroeder, P.A., Crowe P. & Esenli, F. (2013): Origin of the Düvertepe kaolin-alunite deposits in Simav Graben, Turkey: Timing and styles of hydrothermal mineralization. *Jour. Volcan. Geo. Res.*, 255, 57–78.
- Ece, Ö.I. & Schroeder, P.A. (2007): Clay mineralogy and chemistry of halloysite and alunite deposits in the Turplu area, Balıksesir, Turkey. *Clays Clay Minerals* 55, 18–35.
- Frost, R.L. & Shurvell, H.F. (1997): Raman microprobe spectroscopy of halloysite. *Clays Clay Minerals*, 45, 68–72.
- Frost, R.L. & Vassallo, A.M. (1996): The dihydroxylation of the kaolinite clay minerals using infrared emission spectroscopy. *Clays Clay Minerals*, 44, 635–651.

- Frost, R.L., Fredericks, P.M. & Shurvell, H.F. (1996): Raman microscopy of some kaolinite clay minerals. *Can. Jour. Appl. Spectroscopy*, 41, 10–14.
- Frost, R.L. (1995): Fourier transform Raman spectroscopy of kaolinite, dickite and halloysite. *Clays Clay Minerals*, 43, 191–195.
- Frost, R.L. (1998): Hydroxyl deformation in kaolins. *Clays Clay Minerals*, 46, 280–289.
- Fysh, S.A., Cashion, J.D. & Clark P.E. (1983): Mossbauer effect studies of iron in kaolin. I. Structural iron. *Clays Clay Minerals*, 321, 282–292.
- Galán, E. & Martín Vivaldi, J.L. (1973): Caolines españoles. *Geología, mineralogía y génesis. III: Clasificación de los depósitos de caolines españoles según su ambiente genético. Bol. Soc. Esp. Cerámica y Vidrio*, 12, 333–340.
- Gibson, T.G., Bybell, L.M. & Mason, D.B. (2000): Stratigraphic and climatic implications of clay mineral changes around the Paleocene/Eocene boundary of the northeastern US margin *Sedimentary Geology*, 134, 65–92.
- González-López, J.M. (2000): Las arcillas como minerales industriales: caolines, bentonitas y arcillas especiales, *Academia de Ciencias Exactas, Físicas, Químicas y Naturales de Zaragoza*, 7–48.
- Gorbachev, B. F. (1977): Comparative stability and formation conditions of kaolinite and halloysite. *Lithology Min. Resour.*, 12, 700–707.
- Gow, N.N. & Lozej, G.P. (1993): Bauxite. *Geosci. Can.*, 9–16.
- Gruner, J.W. (1932): The crystal structure of kaolinite. *Z. Kristallogr. Kristallgeom.*, 83, 75–88.
- Guggenheim, S. & Eggleton, R.A. (1988): Crystal chemistry, classification, and identification of modulated layer silicates. *Hydrous phyllosilicates. Pp. 675–725 in: Hydrous Phyllosilicates (exclusive of micas) (S.W. Bailey, ed.). Reviews in Mineralogy*, 19, MSA, Chelsea, MI.
- Handley, L., Crouch, E. M. & Pancost, R. D. (2011): A New Zealand record of sea level rise and environmental change during the Paleocene–Eocene Thermal Maximum, *Palaeogeogr. Palaeoclimatol.*, 305, 185–200.
- Hart, R.D., Gilkes, R.J., Siradz, S. & Singh, B. (2002): The nature of soil kaolins from Indonesia and Western Australia. *Clays Clay Minerals*, 50, 198–207.
- Hendricks, S.B. & Teller, E. (1941): X-ray interference in partially ordered layer lattices. *J. chem. Physics.*, 10, 147–167.
- Herbillon, A.J., Mestdagh, M.M., Vielvoye, L. & Derouane, E.G. (1976): Iron in kaolinite with special relevance to kaolinite from tropical soils. *Clay Min.*, 13, 229–235.
- Hong, H., Li, Z. & Xiao, P. (2009): Clay mineralogy along the laterite profile in Hubei, South China: Mineral evolution and evidence for eolian origin. *Clays Clay Minerals*, 57, 5, 602–615.
- Honjo, G., Kitamura, N. & Mihama, K. (1954): A study of clay minerals by means of single-crystal electron diffraction diagrams — the structure of tubular kaolin. *Clay Min. Bull.* 2, 133–141.
- Huertas, F.J., Fiore, S., Huertas, F. & Linares, J. (1999): Experimental study of the hydrothermal formation of kaolinite. *Chem. Geol.*, 156, 171–190.
- Hughes, A.D. & King, M.R. (2010): Use of naturally occurring halloysite nanotubes for enhanced

- capture of flowing cells. *Langmuir*, 26, 12155-12164.
- Inoue, A. (1995): Formation of Clay Minerals in Hydrothermal Environments. Pp. 220–246 In: *Origin in Mineralogy of Clays*, Velde, B. (ed.). Springer. 329 p.
- Inoue, A., Utada, M & Hatta, T. (2012): Halloysite-to-kaolinite transformation by dissolution and recrystallization during weathering of crystalline rocks. *Clay Min.*, 47, 373–390.
- Jeong, G.Y. (2000): The dependence of localized crystallization of halloysite and kaolinite on primary minerals in the weathering profile of granite. *Clays Clay Minerals*, 48, 196–203.
- Jepson, W.B. & Rowse, J.B. (1975): The composition of kaolinite – An electron microscope microprobe study. *Clays Clay Minerals*, 23, 310–317.
- Joussein, E., Petit, S., Churchman, J., Theng, B., Righi, D. & Delvaux, B. (2005): Halloysite clay minerals – A review. *Clay Min.*, 40, 383–426.
- Kamble, R., Ghag, M., Gaikawad, S. & Panda, B.K. (2012): Halloysite nanotubes and applications: A review. *Jour. Adv. Sci. Res.*, 32, 25–29.
- King, R.J. (2009): Kaolinite. *Geology Today*, 25, 75–78.
- Kogure, T. & Inoue, A. (2005): Determination of defect structures in kaolin minerals by high-resolution transmission electron microscopy (HRTEM). *Am. Miner.*, 90, 85–89.
- Kogure, T., Elzea-Kogel, J., Johnston, C.T. & Bish, D.L. (2010): Stacking disorder in a sedimentary kaolinite. *Clays Clay Minerals*, 58, 62–71.
- Kogure, T., Mori, K., Drits, V., Takai, Y. (2013): Structure of prismatic halloysite. *Am. Miner.*, 98, 1008–1016.
- Kohyama N., Fukushima, K. & Fukami, A. (1978): Observation of the hydrated form of tubular halloysite by an electron microscope equipped with an environmental cell. *Clays Clay Minerals*, 26, 25–40.
- Komusinski, J., Stoch, L & Dubiel, S.M. (1981): Application of electron paramagnetic resonance and Mossbauer Spectroscopy in the investigation of kaolinite group minerals. *Clays Clay Minerals*, 18, 261–267.
- Konta, J. (1995): *Clays and Man: Clay Raw Materials in the Service of Man*. *Appl. Clay Sci.*, 10, 275–335.
- Konta, J. (1980): Properties of ceramic raw materials. *Ceramic monographs. Handbook of ceramics*, Schmid-Freiburg, 1–32.
- Lietard, O. (1977): Contribution à l'étude des propriétés physicochimiques, cristallographiques et morphologiques des kaolins. PhD thesis, Nancy, France, 345 pp.
- Liu, M., Guo, B., Du, M., Chen, F. & Jia, D. (2009): Halloysite nanotubes as a novel beta-nucleating agent for isotactic polypropilente. *Polymer*, 50, 3022–3030.
- MacEwan, D.M.C. (1947): The nomenclature of the halloysite minerals. *Miner. Mag.*, 28, 36–44.
- Magasawa, K. & Noro, H. (1987): Mineralogical properties of halloysites of weathering origin. *Chem. Geol.*, 60, 145–149.
- Mansfield, C.F. & Bailey, S.W. (1972): Twin and pseudotwin intergrowths in kaolinite. *Am. Miner.*, 57, 411–425.

- Mehmel, M. (1935): Über die struktur von halloysit und metahalloysit? *Zeitschrift fuer Kristallographie*, 90, 35–42.
- Mendelovici, E., Yarv, S.H. & Villalba, R. (1979): Iron-bearing kaolinite in Venezuelan laterites. I. Infrared spectroscopy and chemical dissolution evidence. *Clay Min.*, 14, 323–331.
- Mestdagh, M.M. Vielvoye, L., Herbillon, A.J. (1980): Iron-bearing kaolinite. II. The relationship between kaolinite crystallinity and iron content. *Clay Min.*, 15, 1–12.
- Mestdagh, M.M., Herbillon, A.J., Rodrique, L. & Rouxhet, P.G. (1982) Évaluation du rôle du fer structural sur la cristallinité des kaolinites. *Bull. Miner.*, 105, 457–466.
- Mingliang, D., Baochun, G. & Demin, P. (2010): Newly emerging applications of halloysite nanotubes: A review. *Polymer Int.*, 59, 5, 574–582.
- Mitra, G.B. & Bhattacharjee, S. (1975): The structure of halloysite. *Acta Crystal.*, B31, 2851–2857.
- Molina, J.M. & Salas, R. (1993): Bauxitas kársticas del Cretácico inferior en Fuentespalda (provincia de Teruel): Estratigrafía, origen y paleogeografía. *Cuad. Geol. Iber.*, 17, 207–230.
- Muhammad, A.S. & Zulfiqar, A. (2008): Geochemistry of the kaolin deposits of Swat (Pakistan). *Chem. der Erde* 68, 207–219.
- Murray, H.H. (1963): Industrial applications of kaolin. *Proc. 10<sup>th</sup> Conf. Clays Clay Minerals*, 291–298.
- Murray, H.H. (1999): Applied clay mineralogy today and tomorrow. *Clay Miner.*, 34, 39–49.
- Nagasawa, K. & Miyazaki, S. (1976): Mineralogical properties of halloysite as related to its genesis. Pp. 257–265 in: *Proceedings of the International Clay Conference 1975* (S.W. Bailey, ed.). Applied Publishing Ltd, Wilmette, USA.
- Nagasawa, K. & Noro, H. (1987): Mineralogical properties of halloysites of weathering origin. *Chem. Geol.*, 60, 145–149.
- Newnham, R.E. (1961): A refinement of dickite structure and some remarks on polymorphism in kaolin minerals. *Mineralog. Mag.*, 32, 683–704.
- Noro, H. (1986): Hexagonal platy halloysite in an altered tuff bed, Komaki city, Aichi prefecture, Central Japan. *Clay Min.*, 21, 401–415.
- Noro, H., Yamada, K. & Suzuki, K. (1981): An application of electron probe microanalysis for clay minerals. *Kobutsugaku Zasshi*, 15, 42–54.
- Parham, W.E. (1969a): Halloysite-rich tropical weathering products of Hong Kong. Pp. 403–416 in: *Proceedings of the International Clay Conference 1969*, Tokyo (L. Heller, ed.). Israel University Press, Jerusalem Tokyo, Japan.
- Parham, W.E. (1969b): Formation of halloysite from feldspar: Low temperature artificial weathering versus natural weathering. *Clays Clay Minerals*, 17, 13–22.
- Pasbakhsh, P. & Churchman, G.J. (2015): *Natural Mineral Nanotubes: Properties and Applications*. Apple Academic Press Inc., Canada, 485 pp.
- Petit, S. & Decarreau, A. (1990): Hydrothermal (200°C) synthesis and crystal chemistry of iron-rich kaolinites. *Clay Min.*, 25, 181–196.
- Price, R.R., Gaber, P.B. & Lvov, Y. (2001): In-vitro release characteristics of tetracycline HCl, khellin and nicotinamide adenine dincucleotide from halloysite; a cylindrical mineral. *Jour.*

- Microencapsulation, 18, 6, 713–722.
- Radoslovich, E.W. (1963): The cell dimensions and symmetry of layer-lattice silicate. VI. Serpentine and kaolin morphology. *Am. Miner.*, 48, 368–378.
- Rengasamy, P., Krishna, G.S.R. & Sarma, V.A.K. (1975): Isomorphous substitution of iron for aluminium in some soil kaolinites. *Clays Clay Minerals*, 23, 211–214.
- Robert, C. & Kennett, J. (1992): Paleocene and Eocene kaolinite distribution in the South Atlantic and Southern Ocean: Antarctic climatic and paleoceanographic implications. *Marine Geol.* 103, 99–110.
- Robertson, I.D.M. & Eggleton, R.A. (1991): Weathering of granitic muscovite to kaolinite and halloysite and plagioclase-derived kaolinite to halloysite. *Clays Clay Minerals*, 39, 113–126.
- Romero, R., Robert, M., Elsass, F. & Garcia, C. (1992): Abundance of halloysite neoformation in soils developed from crystalline rocks. Contribution of transmission electron microscopy. *Clay Min.*, 27, 35–46.
- Ross, C.S. & Kerr, P.F. (1931): The kaolin minerals. Prof. Pap. U.S. geol. Surv, 165-151-180.
- Samotoin, N.D. & Bortnikov, N.S. (2011): Formation of nano- and microcrystals by weathering of phyllosilicates. *Geol. Ore Deposits*, 53, 340–352.
- Schaefer, K. (2008): Cosmetics and Toiletries Special Delivery. In: *Antioxidants and the Skin* (Ed. McMullen, R.L), 500 pp. SBN-13: 9781937235284.
- Schneider, M.A. & Bowen, G.J. (2013): Isotopic ratios and concentrations for mineral-associated and particulate organic fractions of sediment core Wilson Lake samples. doi: 10.1594/PAN-GAEA.824422.
- Singh, B. & Mackinnon, I.D.R. (1996): Experimental transformation of kaolinite to halloysite. *Clays Clay Minerals*, 44, 825–834
- Singh B. (1996): Why does halloysite roll? A new model. *Clays Clay Minerals*, 44, 191–196.
- Singh, B. & Gilkes, R.J. (1992): An electron optical investigation of the alteration of kaolinite to halloysite. *Clays Clay Minerals*, 40, 212–229.
- Stone, W.E.E. & Torres-Sánchez, R.M. (1988): Nuclear magnetic resonance spectroscopy applied to minerals. Part 6. Structural iron in kaolinites as viewed by proton magnetic resonance. *J. Chem Soc., Faraday Trans L* 84, 117–132.
- Sudo, T. (1953): Particle shape of a certain clay of hydrated halloysite, as revealed by electron microscope. *Mineralogical Journal*, 1, 66–68.
- Tari G., Bobos I., Gomes, C.S.F. & Ferreira, J.M.F. (1999): Modification of surface charge properties during kaolinite to halloysite-7 Å transformation. *Jour. Colloid Interface Sci.*, 210, 360–366.
- Tazaki, K. (1979): Micromorphology of halloysites produced by weathering of plagioclase in volcanic ash. Pp. 415–422 in: *Proc. 6<sup>th</sup> Int. Clay Conf. 1978* (M.M.Mortland & V.C. Farmer, eds.). *Developments in Sedimentology*, 27, Elsevier, Amsterdam.
- Tazaki, K. (1982): Analytical electron microscopic studies of halloysite formation processes: Morphology and composition of halloysite. Pp. 573–584 in: *Proc. 7<sup>th</sup> Int. Clay Conf. 1981* (H. Van Olphen & F. Veniale, eds.). *Developments in Sedimentology*, 35, Elsevier.

- Tomura, S., Shibasaki, Y., Mizuta, H. & Kitamura, M. (1985): Growth conditions and genesis of spherical and platy kaolinite. *Clays Clay Minerals*, 33, 200–206.
- Wada, S.I. & Mizota, C. (1982): Iron-rich halloysite (10 Å) with crumpled lamellar morphology from Hokkaido, Japan. *Clays Clay Minerals*, 30, 315–317.
- Ward, C. & Roberts, F.I. (1990): Occurrence of spherical halloysite in bituminous coals of the Sydney basin, Australia. *Clays Clay Minerals*, 38, 501–506.
- Weaver, C.E. (1989): *Clays, muds and shales*. Springer, 787 pp., ISBN: 978-0-444-87381-1.
- White, G.N. & Dixon, J.B. (2002): Kaolin-serpentine minerals. Pp. 389–414 in: *Soil Mineralogy with Environmental Applications* (J.B. Dixon & D.G. Schulze, eds.). Soil Sci. Soc. Am., Madison, Wisconsin.
- Wilke, B.M., Schwertmann, U. & Murad, E. (1978): An occurrence of polymorphic halloysite in granite saprolite of the Bayerischer Wald, Germany. *Clay Min.*, 13, 66–67.
- Wright, P., Taylor, K.G. & Beck, V.H. (2000): The paleohydrology of Lower Cretaceous seasonal wetlands, Isle of Wight, Southern England. *Jour. Sed. Res.*, 70, 3, 619–632.
- Yuste, A., Bauluz, B., Mayayo M.J. (2014): Genesis and mineral transformations in Lower Cretaceous karst bauxites (NE Spain): Climatic influence and superimposed processes. *Geol. Jour.*, DOI: 10.1002/gj.2604.
- Yuste, A., Bauluz, B., Mayayo, M.J. (2013): Mineralogía y textura de las bauxitas kársticas de Fuentespalda (Maestrazgo, Teruel). XXIII Reunión Científica de la SEM. *Macla*, 17, 117–118.